

# Quantum Interfaces Using Nanoscale Surface Plasmons

Fang-Yu Hong and Shi-Jie Xiong

National Laboratory of Solid State Microstructures and Department of Physics, Nanjing University, Nanjing 210093, China

(Dated: November 2, 2018)

The strong coupling between individual optical emitters and propagating surface plasmons confined to a conducting nanotip make this system act as an ideal interface for quantum networks, through which a stationary qubit and a flying photon (surface plasmon) qubit can be interconverted via a Raman process. This quantum interface paves the way for many essential functions of a quantum network, including sending, receiving, transferring, swapping, and entangling qubits at distributed quantum nodes as well as a deterministic source and an efficient detector of a single-photon. Numerical simulation shows that this scheme is robust against experimental imperfections and has high fidelity. Furthermore, being smaller this interface would significantly facilitate the scalability of quantum computers.

PACS numbers: 03.67.-a, 03.67.Hk, 73.20.Mf, 42.50.-p

Keywords: quantum interface, surface plasmon, nanotip

## I. INTRODUCTION

Quantum networks comprised of local nodes and quantum channels are of fundamental importance for quantum communication and essential for scalable and distributed quantum computation [1, 2]. A quantum interface mapping between local and flying qubits is the key component of the quantum network. Schemes for this purpose utilizing strong coupling [3, 4] between a high-Q optical cavity and the atoms have been suggested [5, 6, 7]. However, such schemes put challenging constraints on optical cavities which is difficult to be miniaturized. A novel scheme based on surface plasmons (SPs) to reach the strong-coupling regime on a chip has been intensively explored [8, 9, 10, 11, 12, 13, 14, 15]. A substantial increase in the coupling strength  $g \propto 1/\sqrt{V_{eff}}$  can be achieved through using SPs where the effective mode volume  $V_{eff}$  for the photons can be greatly reduced [13]. An effective Purcell factor  $P \equiv \Gamma_p/\Gamma' \approx 2.5 \times 10^3$  in realistic systems is possible [16], where  $\Gamma_p$  is the spontaneous emission rate into the surface plasmons and  $\Gamma'$  describes the loss rate into other channels. Furthermore, unlike the strong coupling based on cavity quantum electrodynamics (QED), this strong coupling is broadband [13].

On account of these considerations, we propose a general control scheme of emitter-photon quantum interface based on the strong interaction between surface plasmons in a nanotip and an optical emitter. The process of the state transfer between two nodes can be separated into two steps: the sending operation at one node mapping a stationary qubit into a flying qubit and the receiving operation at another node mapping the flying qubit into a stationary one. With the advance in the pulse shaping technique [18], two aspects of the process are controllable: the production of an arbitrarily shaped pulse under the condition that it is sufficiently smooth and the operation of the Raman process as a partial cycle, in which the initial state  $|s\rangle|vac\rangle$  is mapped into an entangled state  $\cos\theta|s\rangle|vac\rangle + \sin\theta|g\rangle|E(t)\rangle$  for any  $\theta \in [0, \pi/2]$ , where  $|g\rangle$  and  $|s\rangle$  are the stationary qubit states and the flying qubit is denoted by the vacuum state  $|vac\rangle$  and a single plasmon (pho-

ton) state with wave packet  $|E(t)\rangle$ .

A number of essential functions of a quantum network can be fulfilled by this quantum interface: (i) It can send a flying quantum state and can also function as a deterministic source of a single photon with arbitrary pulse shape and controllable average photon number. (ii) It can receive a flying quantum state [19], being an efficient single-photon detector if the incoming photon pulse shape is known. (iii) A state can be transferred from one node to another. (iv) An entanglement between either two remote stationary qubits or a stationary qubit and a flying qubit can be generated in a partial Raman cycle. Numerical simulations of this scheme demonstrate robustness against parameters errors and high fidelity. With stronger emitter photon coupling strength, faster manipulation times can be expected. Furthermore, as the setup is much easier to be made smaller, this scheme would open the possibility to higher scalability of quantum computers.

## II. EXACT SOLUTION OF THE QUANTUM INTERFACE DYNAMICS

The prototype quantum interface consists of a nanotip and a three-level emitter [12, 14, 15, 16] described by the operator  $\sigma_{ij} = |i\rangle\langle j|$ ,  $i, j = e, g, s$  (Fig.1). Here, the qubit is represented by a ground state  $|g\rangle$  and a metastable state  $|s\rangle$ . State  $|s\rangle$  is decoupled from the surface plasmons owing to, for example, a different orientation of its associated dipole moment [13], but is resonantly coupled to excited  $|e\rangle$  via some classical, optical control field  $\Omega(t)$  with central frequency  $\omega_L$ . States  $|g\rangle$  and  $|e\rangle$  is coupled with strength  $g$  via the surface plasmon modes with wave vector  $k$  which is described by annihilation operation  $a_k$ . States  $|g\rangle$ ,  $|s\rangle$ , and  $|e\rangle$  have the energy  $\omega_g = 0$ ,  $\omega_s$ , and  $\omega_e$ , respectively. The laser light satisfies the resonance condition:  $\omega_L + \omega_s = \omega_e$ . Since the coupling  $g$  is broad-band, it can be assumed to be frequency-independent [13, 16]. A linear dispersion relation  $\omega_k = c|k|$  holds provided  $\hbar\omega_k < 2$  eV [15, 17], with  $c$  denoting the group velocity of the SPs. Then similar to the Hamiltonian in [13] describing the interaction of an emitter and a nanowire, the Hamiltonian for our model

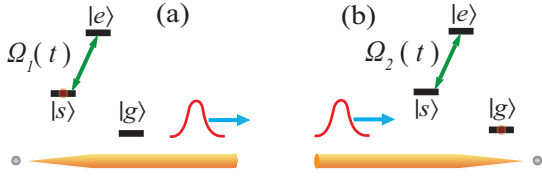


FIG. 1: (Color online) Schematic picture of the interface comprised of an optical emitter and a nanotip for the quantum network. (a) The interface for sending process. A three-level optical emitter starts in state  $|s\rangle$ , is coupled to excited state  $|e\rangle$  via a time-dependent external control field  $\Omega_1(t)$ . We assume that the excited state  $|e\rangle$  is coupled to state  $|g\rangle$  via the plasmon modes, causing  $|e\rangle$  to decay into  $|g\rangle$  with high probability, while simultaneously generating a single-photon in the plasmon modes. The control pulse  $\Omega_1(t)$  is determined by the shape of the generated photon wave packet which can be arbitrarily specified. (b) The interface for receiving process. The emitter is initially in the ground state  $|g\rangle$ . Under the action of  $\Omega_2(t)$  which is determined by the wave packet of the incoming photon, the emitter can absorb a photon while inducing a state flip from  $|g\rangle$  to  $|s\rangle$ .

can be written in the form

$$H = (\omega_e - i\frac{\Gamma'}{2})\sigma_{ee} + \omega_s\sigma_{ss} - (\Omega(t)e^{-i\omega_L t}\sigma_{es} + H.c.) + \int_{-\infty}^{\infty} dk c|k|a_k^\dagger a_k - (g \int_{-\infty}^{\infty} dk \sigma_{eg} a_k + H.c.), \quad (1)$$

where the emitter is assumed to be in the origin of an axis and the non-Hermitian term in  $H$  describes the decay of state  $|e\rangle$  at a rate  $\Gamma'$  into all other possible channels [12]. This effective hamiltonian is in effect under the condition that  $k_B T \ll \hbar\omega_e$ , e.g., if  $\hbar\omega_e = 1$  meV,  $T < 1$  K, where  $k_B$  is the Boltzmann constant [13].

Note that the system described by this Hamiltonian, has two invariant Hilbert subspaces, with the bases  $\{|g, vac\rangle\}$  and  $\{|s, vac\rangle, |e, vac\rangle, |g, k\rangle\}$ , respectively (where in  $|m, n\rangle$ ,  $m = g, s, e$  denotes the state of three-level system and  $|k\rangle$  denotes the one-photon Fock state of the surface plasmon mode of wave vector  $k$ ). So the evolution of the system containing one excitation can be generally described by the state  $|\Psi(t)\rangle = \alpha_g|g, vac\rangle + \alpha_s|\psi(t)\rangle$ , where

$$|\psi(t)\rangle = \int_{-\infty}^{\infty} dk \beta_k(t) a_k^\dagger |g, vac\rangle + \beta_e(t) |e, vac\rangle + \beta_s(t) |s, vac\rangle. \quad (2)$$

Under the Hamiltonian given in equation (1), the equations of motion for the resonant Raman process (in a rotation frame) can be derived as

$$\dot{\beta}_k(t) = -i\delta_k \beta_k(t) + ig\beta_e(t), \quad (3)$$

$$\dot{\beta}_e(t) = -\frac{\Gamma'}{2}\beta_e(t) + i\Omega(t)\beta_s(t) + ig \int_{-\infty}^{\infty} dk \beta_k(t). \quad (4)$$

where  $\delta_k = c|k| - \omega_e$ . Integrating equation (3) yields

$$\beta_k(t) = \beta_k(-\infty)e^{-i\delta_k t} + ig \int_{-\infty}^t dt' \beta_e(t') e^{-i\delta_k(t-t')}, \quad (5a)$$

$$= \beta_k(\infty)e^{-i\delta_k t} - ig \int_t^{\infty} dt' \beta_e(t') e^{-i\delta_k(t-t')}. \quad (5b)$$

Equations (5a) can be used for the receiving process, while equation (5b) for the sending process. Substituting equations (5) into equation (4), within the Wigner-Weisskopf approximation [13, 20], we have the equations of motion for the atomic state:

$$\dot{\beta}_e(t) = i\Omega(t)\beta_s(t) - \frac{\Gamma_p + \Gamma'}{2}\beta_e(t) + i\sqrt{2\pi}gE_{in}(t), \quad (6a)$$

$$= i\Omega(t)\beta_s(t) - \frac{-\Gamma_p + \Gamma'}{2}\beta_e(t) + i\sqrt{2\pi}gE_{out}(t), \quad (6b)$$

$$\dot{\beta}_s(t) = i\Omega^*(t)\beta_e(t), \quad (6c)$$

where  $\Gamma_p = 2\pi g^2/c$  is the spontaneous emission rate into the SP modes,

$$E_{in}(t) = 1/\sqrt{2\pi} \int_{-\infty}^{\infty} dk \beta_k(-\infty) e^{-i\delta_k t} = 1/\sqrt{2\pi} \int_0^{\infty} dk \beta_k(-\infty) e^{-i\delta_k t}, \quad (7)$$

and  $E_{out}(t) = 1/\sqrt{2\pi} \int_{-\infty}^0 dk \beta_k(\infty) e^{-i\delta_k t}$  are the incoming and outgoing single-photon wave functions (in a rotating frame), respectively. We have assumed that  $\beta_k(-\infty) = 0$  if  $k < 0$  for the incoming field and  $\beta_k(\infty) = 0$  if  $k > 0$  for the outgoing field.

Below we will show that, from equations (6), the amplitudes  $\beta_e(t)$  and  $\beta_s(t)$  including the control pulse  $\Omega(t)$  can be expressed in terms of  $E_{in}(t)$  and  $E_{out}(t)$ . Thus the desired operation, with  $E_{in}(t)$  and  $E_{out}(t)$  arbitrarily specified, can be generated on demand as long as the normalization of the wave function of equation (2) is satisfied. From equations (6a),(6b), we have

$$\beta_e(t) = \frac{ic}{\sqrt{2\pi}g}(E_{in} - E_{out}). \quad (8)$$

From equations (6), we can solve for the amplitude of  $\beta_s(t)$ :

$$\frac{d}{dt}|\beta_s(t)|^2 = c(|E_{in}(t)|^2 - |E_{out}(t)|^2) - \frac{c}{P}|E_{out}(t) - E_{in}(t)|^2 - \frac{c}{\Gamma_p} \frac{d}{dt}|E_{out}(t) - E_{in}(t)|^2 \quad (9)$$

and the phase:

$$\frac{d\theta}{dt} = \frac{i}{|\beta_s(t)|^2} \left[ \beta_e(t) \left( \frac{d}{dt}\beta_e^*(t) + \frac{\Gamma_p + \Gamma'}{2}\beta_e^*(t) + i\sqrt{2\pi}gE_{in}^*(t) \right) + \frac{1}{2} \frac{d}{dt}|\beta_s(t)|^2 \right]. \quad (10)$$

Then, from equation (6c), we can express  $\Omega(t)$  in terms of the amplitudes that have been solved above:

$$\Omega(t) = i \left( \frac{d}{dt}\beta_s^*(t) \right) / \beta_e^*(t). \quad (11)$$

For the sending node of the quantum network, the initial conditions are  $E_{in}(t) = 0$ ,  $\beta_e(-\infty) = 0$ , and  $\beta_s(-\infty) = 1$ .

The outgoing single-photon wave packet can contain average  $\sin^2 \theta$  photon:  $\int_{-\infty}^{\infty} d\tau |E_{out}(\tau)|^2 = \sin^2 \theta \int_{-\infty}^{\infty} d\tau |\tilde{E}_{out}(\tau)|^2 = \sin^2 \theta/c$ , where  $\tilde{E}_{out}(t)$  is the normalized wavepacket of the emitted photon. At the remote future time  $t \rightarrow +\infty$ , the photon emission process is completed, we have  $\beta_e(t) = 0$ , and  $\beta_s(t) = (1 - (1 - 1/P) \sin^2 \theta)^{1/2} e^{i\phi} \approx \cos \theta e^{i\phi}$ , with the controllable phase given by equation (10). The most general form of the photon generation process can be described by

$$\begin{aligned} \alpha_g |g, vac\rangle + \alpha_s |s, vac\rangle &\xrightarrow{\Omega(t)} \alpha_g |g, vac\rangle \\ &+ \alpha_s [e^{i\phi} \cos \theta |s, vac\rangle + \sin \theta |g, \tilde{E}_{out}(t)\rangle] \end{aligned} \quad (12)$$

If  $\theta = \pi/2$  and equation (12) is reduced to the equation

$$(\alpha_g |g\rangle + \alpha_s |s\rangle) |vac\rangle \rightarrow |g\rangle (\alpha_g |vac\rangle + \alpha_s |\tilde{E}_{out}(t)\rangle). \quad (13)$$

mapping the stationary qubit onto the flying qubit. Further, if initially the emitter is entirely in state  $|s\rangle$ , then this mapping operation can work as the deterministic generation of a single-photon wave packet with any desired pulse shape  $\tilde{E}_{out}(t)$ . If  $\theta < \pi/2$ , this sending node can also function as generation of entanglement between the emitter and the flying qubit:

$$|s, vac\rangle \xrightarrow{\Omega(t)} e^{i\phi} \cos \theta |s, vac\rangle + \sin \theta |g, \tilde{E}_{out}(t)\rangle. \quad (14)$$

The receiving process is basically the time reversal of the full-cycle sending process. With the emitter initially in state  $|g\rangle$  and the incoming flying qubit  $\alpha_g |vac\rangle + \alpha_s |\tilde{E}_{in}(t)\rangle$ , the mapping transformation is expressed by

$$|g\rangle (\alpha_g |vac\rangle + \alpha_s |\tilde{E}_{in}(t)\rangle) \rightarrow (\alpha_g |g\rangle + \alpha_s |s\rangle) |vac\rangle. \quad (15)$$

As in the sending process, the incoming photon pulse  $\tilde{E}_{in}(t)$  photon can be arbitrarily specified, provided that it is smooth enough and without the outgoing photon. As the stationary qubit can be read out non-destructively [21, 22], the receiving node can also function as a photon detector when the photon pulse shape is known.

By combining the sending and receiving process, the transfer of qubit from one node to another can be easily accomplished. When two state transfer operations with opposite directions are performed at the same time, the two qubits are swapped. If  $\theta < \pi/2$ , the joint operation of the sending and receiving process can produce an entangled state of the two nodes by the transformation:

$$|s, g\rangle |vac\rangle \xrightarrow{\Omega_1(t), \Omega_2(t)} (e^{i\phi} \cos \theta |s, g\rangle + \sin \theta |g, s\rangle) |vac\rangle. \quad (16)$$

Before surface plasmons decay they can travel about 140 plasmon wavelengths [12] which corresponding to about 0.2 m for the energy split  $\omega_{eg} = 1$  meV and dielectric permittivity  $\epsilon = 50$  [12]. Thus, the loss of the SP during the travel can be negligible if the two node is about 1  $\mu\text{m}$  apart from each other. In our model, the difference in energy levels between the two emitters in the two nodes can be allowed to exist, thus in the realistic systems, the two emitter can be independently addressed and the effect that a close spacing between

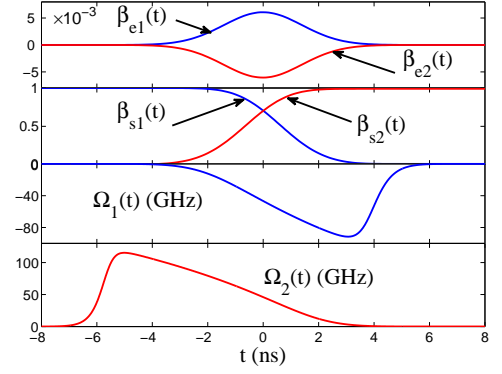


FIG. 2: (Color online) Transfer of a qubit from the sending node to the receiving node. (a) Amplitudes of the state  $\beta_{e1}$  and  $\beta_{e2}$ . (b) Amplitude of the states  $\beta_{s1}$  and  $\beta_{s2}$ . (c) The control field  $\Omega_1(t)$  for the sending process. (d) The control field  $\Omega_2(t)$  for the receiving process.

two atom affects the spontaneous emission process [23] can be suppressed. Short distance quantum communications are essential for a quantum computer. For long distance communications, the SPs can be in- and out-coupled to conventional waveguides [13].

### III. NUMERICAL SIMULATIONS

In the following numerical simulations, for simplicity we assume that  $E_{1out}(t - \tau) = E_{2in}(t)$  with  $\tau$  denoting the propagation delay and the corresponding parameters for the sending and receiving nodes are same. Assuming  $g = 1.6 \times 10^{10} \text{ m}^{1/2} \text{ s}^{-1}$ ,  $P = 100$ ,  $\tilde{E}_{out}(t) = i \sqrt{\frac{\sqrt{2}}{a\sqrt{\pi}}} e^{-(ct/a)^2} m^{-1/2}$  with  $c = 1.5 \times 10^8 \text{ m/s}$  and  $a = 0.3 \text{ m}$ , we illustrate the transfer of a qubit from node 1 to node 2 by the mapping transformation  $(\alpha_g |g\rangle + \alpha_s |s\rangle) |g\rangle \rightarrow |g\rangle (\alpha_g |g\rangle + 0.9950 \alpha_s |s\rangle)$  with  $\beta_{s1}(\infty) = 0.0095$ . The fidelity of this operation is  $F = 0.9900$  for the transferred state with coefficients  $\alpha_g = \alpha_s = 1/\sqrt{2}$ . If  $P = 1000$  with other parameters unchanged, we have  $F = 0.9990$ . Using the same parameters as those used in the figure 2, we present in figure 3 the creation of entanglement of the qubits in neighboring nodes through the transformation:  $|s, g\rangle \rightarrow 0.7047 |s, g\rangle + 0.7004 |g, s\rangle$ . The target mapping is  $|s, g\rangle \rightarrow 1/\sqrt{2} (|s, g\rangle + |g, s\rangle)$ , so the fidelity of this operation is  $F = 0.987$ . Note that in the receiving node, the control field  $\Omega_2(t)$  must be designed to absorb a whole photon, no matter whether the incoming field contains a whole photon or not. Otherwise, the operation of either the state transfer or the generation of entanglement between two nodes will yield wrong result.

In the above analysis, exact knowledge of the parameters is assumed. Table I shows the effect of the unknown errors in the various parameters on the fidelity of the transfer of a qubit from the sending node to the receiving one. From Table I, we see that the scheme is robust against experimental imper-

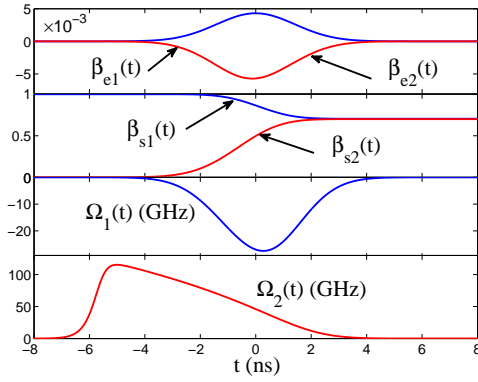


FIG. 3: (Color online) Generation of entanglement of two qubits in neighboring nodes with the target state:  $(|s, g\rangle + |g, s\rangle) / \sqrt{2}$ . (a) Amplitude of the states  $\beta_{e1}$  and  $\beta_{e2}$ . (b) Amplitude of the states  $\beta_{s1}$  and  $\beta_{s2}$ . (c) The driving field  $\Omega_1(t)$  for the sending process. (d) The driving field  $\Omega_2(t)$  for the receiving process.

TABLE I: Effect of errors in parameters on the fidelity of state transfer operations. The parameters remain the same as those used in figure 2. When there are no errors, the fidelity  $F = 0.9900$ .

node1	10% $g$ err	10% $\Gamma_{pl}$ err	10% $\Gamma'$ err	10% $\Omega_1(t)$ err
Fidelity	0.8910	0.9429	0.9895	0.9845
node2	10% $g$ err	10% $\Gamma_{pl}$ err	10% $\Gamma'$ err	10% $\Omega_2(t)$ err
Fidelity	0.8940	0.9426	0.9895	0.9840

fections except the uncertainty in coupling  $g$  and the resulting  $\Gamma_{pl} = 2\pi g^2/c$ , which can be overcome, since the position of the emitter on which the coupling  $g$  is dependent [16] can be determined with very high accuracy.  $\Omega(t)$  can also have unknown phase error due to laser fluctuation which can be considered static in the time scale of ns. The problem resulting from the relative phase between  $\Omega_1(t - \tau)$  and  $\Omega_2(t)$  can be solved by employing a delayed phase locking of the control field in the two nodes [7].

#### IV. CONCLUSION

We have shown a general and exact solution for the dynamics of a quantum interface consisting of a three-level optical emitter coupled to a proximal nanotip. The scheme enables many essential quantum network operations including sending, receiving, swapping, and entangling qubit at distant nodes to be performed with near unity fidelity and in a shorter operation time than those based on the cavity QED. Furthermore, the setup is easier to be miniaturized, thus would significantly facilitate the scalability of quantum computers. This scheme is applicable to a wide range of physical implementations of quantum interface such as solid state systems [24], trapped ions [25] and ultrasmall quantum dots [26, 27] with discrete levels and in particular with electron spin levels.

#### ACKNOWLEDGMENTS

This work was supported by the State Key Programs for Basic Research of China (2005CB623605 and 2006CB921803), and by National Foundation of Natural Science in China Grant Nos. 10474033 and 60676056.

- [1] J.I. Cirac, A.K. Ekert, S.F. Huelga, and C. Macchiavello, Phys. Rev. A **59**, 4249 (1999).
- [2] D. DiVincenzo, Fortschr. Phys. **48**, 771 (2000).
- [3] R.J. Thompson, G. Rempe, and H.J. Kimble, Phys. Rev. Lett. **68**, 1132 (1992).
- [4] M. Brune *et al.*, Phys. Rev. Lett. **76**, 1800 (1996).
- [5] J.I. Cirac, P. Zoller, H.J. Kimble, and H. Mabuchi, Phys. Rev. Lett. **78**, 3221 (1997).
- [6] L.-M. Duan, A. Kuzmich, and H. J. Kimble, Phys. Rev. A **67**, 032305 (2003).
- [7] W. Yao, R.-B. Liu, and L.J. Sham, Phys. Rev. Lett. **95**, 030504 (2005).
- [8] L. Childress, A.S. Sørensen, and M.D. Lukin, Phys. Rev. A **69**, 042302 (2004).
- [9] A.S. Sørensen *et al.*, Phys. Rev. Lett. **92**, 063601 (2004).
- [10] A. Blais *et al.*, Phys. Rev. A **69**, 062320 (2004).
- [11] A. Wallraff *et al.*, Nature (London) **431**, 162 (2004).
- [12] D.E. Chang, A.S. Sørensen, P.R. Hemmer, and M.D. Lukin, Phys. Rev. Lett. **97**, 053002 (2006).
- [13] D.E. Chang, A.S. Sørensen, E.A. Demler, and M.D. Lukin, Nat. Phys. **3**, 807 (2007).
- [14] M.I. Stockman, Phys. Rev. Lett. **93**, 137404 (2004).
- [15] C. Ropers, C.C. Neacsu, T. Elsaesser, M. Albrecht, M.B. Raschke, and C. Lienau, Nano Lett. **7**, 2784 (2007).
- [16] D.E. Chang, A.S. Sørensen, P.R. Hemmer, and M.D. Lukin, Phys. Rev. B **76**, 035420 (2007).
- [17] G. Schider, J.R. Krenn, A. Hohenau, H. Dittlbacher, A. Leitner, F.R. Aussenegg, W.L. Schaich, I. Puscasu, B. Monacelli, and G. Boreman, Phys. Rev. B **68**, 155427 (2003).
- [18] D.B. Strasfeld, S.-H. Shim, and M.T. Zanni, Phys. Rev. Lett. **99**, 038102 (2007).
- [19] I. Novikova, A.V. Gorshkov, D.F. Phillipps, A.S. Sørensen, M.D. Lukin, and R.L. Walsworth, Phys. Rev. Lett. **98**, 243602 (2007).
- [20] P. Meystre and M. Sargent III, Elements of Quantum Optics 3rd edn (Springer, New York, 1999).
- [21] R.B. Liu, W. Yao, and L.J. Sham, Phys. Rev. B **72**, 081306 (2005).
- [22] M.J. Testolin, A.D. Greentree, C.J. Wellard, and L.C.L. Hollenberg, Phys. Rev. B **72**, 195325 (2005).
- [23] R.H. Lehberg, Phys. Rev. A **2**, 889 (1970).
- [24] B.E. Kane, Nature **393**, 133 (1998).
- [25] J.F. Poyatos, J.I. Cirac and P. Zoller, Fortschr. Phys. **48**, 785 (2000).
- [26] D. Loss and D.P. DiVincenzo, Phys. Rev. A **57**, 120 (1998).
- [27] G. Burkard, H.-A. Engel and D. Loss, Fortschr. Phys. **48**, 965 (2000).
- [28] K.P. Nayak, P.N. Melentiev, M. Morinaga, F.L. Kien, V.I. Balykin, and K. Hakuta, Opt. Express **15**, 5431 (2007).